COMPARISON OF REACTIVITY OF SYNTHETIC AND BOVINE HYDROXYAPATITE *IN VITRO* UNDER DYNAMIC CONDITIONS

#DIANA HORKAVCOVÁ, DANA ROHANOVÁ, LENKA KUNCOVÁ, KLÁRA ZÍTKOVÁ, ZUZANA ZLÁMALOVÁ CÍLOVÁ, ALEŠ HELEBRANT

Department of Glass and Ceramics, Institute of Chemical Technology, Technická 5, 166 28 Prague 6, Czech Republic

#E-mail: diana.horkavcova@vscht.cz

Submitted October 5, 2013; accepted March 4, 2014

Keywords: Hydroxyapatite, in vitro test, SBF

Hydroxyapatite materials prepared by two methods: synthetic (HA–S) and bovine (HA-B) granules were exposed to a long-term in vitro test under dynamic conditions. Testing cells, filled up to one fourth (¼V) of their volume with the tested material, were exposed to continuous flow of simulated body fluid (SBF) for 56 days. The objective of the experiment was to determine whether reactivity of the biomaterials (hydroxyapatites), prepared by different methods but identical in terms of their chemical and phase composition, in SBF were comparable. Analyses of the solutions proved that both materials were highly reactive from the very beginning of interaction with SBF (significant decrease of Ca^{2+} and $(PO_4)^{3-}$ concentrations in the leachate). SEM/EDS images have shown that the surface of bovine HA-B was covered with a new hydroxyapatite (HAp) phase in the first two weeks of the test while synthetic HA–S was covered after two weeks of the immersion in SBF. At the end of the test, day 56, both materials were completely covered with well developed porous HAp phase in form of nano-plates. A calculation of the rate of HAp formation from the concentration of $(PO_4)^{3-}$ ions in SBF leachates confirmed that all removed ions were consumed for the formation of the HAp phase throughout the entire testing time for bovine HA–B and only during the second half of the testing time for synthetic HA–S.

INTRODUCTION

Bioactive materials based on calcium phosphates have been widely used in medicine, particularly in dental surgery. The materials may be in form of micro- or macro-porous granules, scaffolds, cements etc. After their implantation biochemical reactions occur at the interface between the implant and bone tissue which result in formation of a mechanically strong interconnection with a layer of precipitated hydroxyapatite - the so-called bioactive fixation [1-4]. The bioactive materials include glass, bioactive glass ceramics and ceramics based on calcium phosphates. The material most frequently used in calcium-phosphate ceramics is hydroxyapatite HA ($Ca_{10}(PO_4)_6(OH)_2$) because its chemical composition is similar to the mineral part of bone and teeth tissue. Another calcium-phosphate ceramics used in practice is tricalcium phosphate β-TCP ($Ca_3(PO_4)_2$) [1-4]. Much attention has been paid to the synthesis of calcium phosphates, particularly hydroxyapatite, while seeking preparation of a high-purity nano- to micro-crystalline product, which is stable in solutions with pH above 4.2. Basic methods of preparation of synthetic hydroxyapatites include chemical precipitation through aqueous solution [5-8], sol-gel method [9-11], mechanochemical process [8, 12, 13] or solid-state sintering process [14]. Other options include preparation of bovine hydroxyapatite from natural bovine bone by a sequence of thermal processes [15] or by annealing and sintering of bovine bone [16, 17]. An important feature of the prepared hydroxyapatites is their resorption and kinetics of solubility in water solutions. The processes can be described with several mechanisms [18], mainly a diffusion model (transport of mass) and reaction on the hydroxyapatite surface [19, 20]. Kinetics of the dissolution is affected primarily by pH and oversaturation of the solution.

Bioactivity of materials can be tested *in vivo* (in live organisms) or *in vitro* (by means of model body fluids). The tests result in formation of a biologically active hydroxyl-carbonate apatite layer on the surface of bioactive implants [1, 2]. Model solution used most frequently for *in vitro* testing is the so-called simulated body fluid (SBF) designed by Kokubo [21]. Ion composition of SBF is similar to the inorganic component of blood plasma and its pH is maintained by means of the TRIS buffer (tris-hydroxymethyl aminomethane) [22]. *In vitro* tests (monitoring kinetics of formation of the apatite phase in simulated body fluid) may be affected both by the material itself (its granulometry, porosity, firing temperature) and by the testing conditions (static or dynamic exposure of the material to SBF, pH value) [23-27]. Essential factors for incorporation of calcium-

phosphate-ceramics-based bioactive materials include not only the rate of intergrowing with the surrounding tissue but also the level of their transformation into a new form of hydroxyapatite phase (HAp).

The first objective of the submitted paper was to compare HAp growth kinetics on the surface of synthetic (HA–S) and bovine (HA–B) micro- and macro-porous granulated hydroxyapatites in the course of their long-term interaction with simulated body fluid under dynamic conditions. The measured increases of weight of the materials and relevant concentrations of phosphates in leachates were used to calculate the growth rate of the new HAp phase. The second objective was to monitor the level of resorption of the tested materials into the new phase of the hydroxyapatite (HAp).

EXPERIMENTAL PART

The micro- and macro-porous apatite materials used in the tests were designed for replacement of bone tissue and made by Lasak Ltd. and by Geistlich Pharma AG. In the former case (Lasak Ltd.) the material was synthetic hydroxyapatite (HA–S, $Ca_{10}(PO_4)_6(OH)_2$) in the form of white granules with the diameter of 1 - 2 mm. Porosity of the granules ranged from 60 to 70 %. In the latter case (Geistlich Pharma AG.) the tested bovine hydroxyapatite (HA–B, $Ca_{10}(PO_4)_6(OH)_2$) was prepared from a mineral component of bovine bone in the form of spongious bone granulate, with the granule size of 1-2 mm. The materials were identified as follows: HA–S 14d, HA–B 14d, HA–S 28d, HA–B 28d, HA–S 42d, HA–B 42d and HA–S 56d, HA–B 56d.

The model fluid used for *in vitro* testing has an ion composition is similar to the inorganic component of blood plasma; this is a frequently used one as designed by Kokubo [21-23]. The simulated body fluid (SBF) was prepared by mixing of solutions of the following reagents: KCl, NaCl, $NaHCO_3$, $MgSO_4.7H_2O$, $CaCl_2$, KH_2PO_4 in appropriate ratios. SBF was buffered with TRIS (Tris-hydroxymethyl aminomethane) and HCl to achieve pH = 7.45. Azide (NaN_3) was added to prevent bacteria growth in the solution [25, 26] during the long-term test.

The long-term interaction of the materials with SBF was monitored under dynamic conditions in order to simulate as close as possible the flow conditions of extracellular fluid in a human organism and the materials were continually exposed to "fresh" SBF. Both the materials were weighed into individual testing cells to fill ¼ of their volumes. Previous work [26] has shown that this filling is optimal for the monitoring of interaction of the material with the solution. The SBF is continually pumped by a peristaltic pump from a supply bottle into four testing cells (with volume 5.5 ml). The flow rate of the solution was approximately at 48 ml per day.

The cells with the tested material were placed in a thermostat set at 36.5 ± 0.5°C. Subsequently, SBF leachates were collected from each of the cells in accurately specified intervals to determine the concentrations of Ca^{2+} and $(PO_4)^{3-}$ ion and to measure the pH values. Every two weeks (on days 14, 28, 42 and 56) one cell was disconnected and the material was examined.

EXPERIMENTAL

The surface of the tested materials before and after the interaction was monitored with (SEM) Hitachi S-4700 electron microscope with EDS analyzer (NORAN D-6823) using the accelerating voltage of 15 kV. The material was coated with a layer of Au-Pd for 80 s.

Diffraction patterns were collected with a PANalytical X´Pert PRO diffractometer equipment with a conventional X-ray tube (CuKα radiation, 40 kV, 30 mA, point focus) and a position-sensitive PIXcel detector with an anti-scatter shield. X-ray patterns were measured in the 2θ range of 10 - 100°, with steps of 0.0131° and 200 s counting per step. Quantitative analysis was performed with the HighScorePlus software package (PANalytical, the Netherlands, version 2.2.5), DiffracPlus software package (Bruker AXS, Germany, version 8.0) and JCPDS PDF-2 database (International Centre for Diffraction Data, Newtown Square, PA, USA) release 54,2004 (in the Institute of Inorganic Chemistry of the Czech Academy of Science, Řež u Prahy). The specific surface of the materials before and after the interaction was determined using the BET method using ASAP 2020 analyzer by Micromeritic, using N_2; temperature 60 - 200°C, heating rate 10°C/min, time at temperature 600 - 2000 min.

The concentration of Ca^{2+} ions in the leachate was analyzed by atomic absorption spectrometry using VARIAN - Spectr AA 300. Atomization was performed in acetylene-N_2O flame. The wavelength used for absorbance measurements was 422.7 nm. The content of $(PO_4)^{3-}$ ions was analyzed on UV-VIS Spectrophotometer UV1601 at $\lambda = 830$ nm under ČSN 830540. Concentrations of both the ions were calculated using a calibration curve from the measured absorbance values. pH values in leachates were measured with inoLab pH-meter with a combined glass electrode at the laboratory temperature.

Calculation of the rate of formation of the new HAp phase on the surface of synthetic and bovine hydroxyapatite

Due to the use of the TRIS buffer in SBF, which can incorporate Ca^{2+} ions into its structure [26, 27], the calculation of the rate of formation of the new HAp phase on the surface of both the materials used values of $(PO_4)^{3-}$

concentrations. The rate of precipitation of the new HAp phase on the surface of HA–S, HA–B was calculated from the actual increase of weight (R_m, equation (3)) and from the decrease of the $(PO_4)^{3-}$ concentration in SBF leachates from the beginning of the interaction (R_c). It is assumed that all $(PO_4)^{3-}$ ions removed from SBF are used for the formation of HAp phase.

$$\Delta m' = [(m_t - m_0)\cdot 100]/m_0\ (\%) \quad (1)$$

$$\Delta S' = [(S_t - S_0)\cdot 100]/S_0\ (\%) \quad (2)$$

$$R_m = (m_t - m_0)/t\ (\mathrm{mg\cdot hour^{-1}}) \quad (3)$$

$$m_{c(t)} = (c_0 - c_t)\cdot (M_{HAp}/6\cdot M_{(PO4)3-})\cdot F\cdot \Delta t + m_{c(t-\Delta t)}\ (\mathrm{mg}) \quad (4)$$

$$A_{\mathrm{HA-S}} = m_{0\,\mathrm{HA-S}}\cdot S_{0\,\mathrm{HA-S}}\ (\mathrm{m^2}) \quad (5)$$

$$A_{\mathrm{HA-B}} = m_{0\,\mathrm{HA-B}}\cdot S_{0\,\mathrm{HA-B}}\ (\mathrm{m^2}) \quad (6)$$

where m_t, m_0 are the weights of the material at the time t and at the beginning of the interaction respectively, rm' is a change of the weight of the material at the time t in percentages, t is the time of the interaction of the material with SBF, S_t, S_0 are the specific surfaces of the material at the time t and at the beginning of the interaction respectively, rS' is a change of the specific surface of the material at the time t in percentages, rt is the time between two collections of SBF leachate samples, R_m is the rate of formation of the new HAp phase calculated from the increase of the material weight, c_t, c_0 are the concentrations of $(PO_4)^{3-}$ ions in SBF at the time t and at the beginning of the interaction respectively, $m_{c(t)}$, $m_{c(t-rt)}$ is the weight of the newly formed HAp calculated from the quantity of $(PO_4)^{3-}$ ions at the respective time, M_{HAp}, $M_{(PO4)3-}$ are the molar weights of HAp and $(PO_4)^{3-}$ respectively, F is the flow rate of SBF (48 ml.day^{-1}), R_c is calculated from tangent of the linear fit of $m_{c(t)}$ time dependence from Figure 4 (HA–S) or Figure 7 (HA–B), A is the original surface area of the material.

RESULTS AND DISCUSSION

Synthetic hydroxyapatite HA–S

Table 1 shows the weight of material HA–S before and after the interaction with SBF. The results indicate that the weight of material slowly grows with the growing time of interaction with SBF. By the end of the interaction the weight increased in total by 69.4 %.

Table 1. The weights of material HA–S before and after 14, 28, 42 and 56 days of interaction with SBF.

Material	Weight (g)		$\Delta m_{\mathrm{HA-S}}$ (g)	$\Delta m'_{\mathrm{HA-S}}$ (%)
	before interaction	after interaction		
HA–S 14d	0.500	0.612	+0.112	+22.4
HA-S 28d	0.500	0.698	+0.198	+39.6
HA-S 42d	0.500	0.761	+0.261	+52.2
HA-S 56d	0.500	0.847	+0.347	+69.4

Changes on the surface of the HA–S material after the interaction with SBF are visible in Figures 1b-e. Figure 1a shows the material before the interaction.

Figures 1b-e show the changes of HA–S morphology as a result of formation of a new hydroxyapatite phase (HAp) on its surface. Formation of the new phase on the surface of the original material is obvious as early as after 14 days of interaction with SBF (Figure 1b) and after 28 days of the interaction (Figure 1c) plates of nano-crystals of the new HAp phase can be observed. With the growing time of interaction the newly formed HAp phase becomes more developed (Figure 1d-e). Using a detailed image of a crack that developed due to drying (Figure 1f) we were able to determine the thickness of the new HAp phase (ca. 30 μm) after 56 days of interaction.

During the first 14 days of interaction with SBF there was an obvious decrease of the specific surface HA–S (Table 2). The trend was recorded throughout the entire time of interaction. Measurements of specific surface have confirmed that the newly developing HAp phase filled the macro- and micro-pores of HA–S and gradually covered the entire surface, as indicated by SEM images. We estimate that after approximately 28 days the original synthetic material HA–S no longer reacts with SBF but probably the newly developed HAp phase.

Table 2. The values of the specific surface of material HA–S before and after 14, 28, 42 and 56 days of interaction with SBF.

Material	Specific surface ($\mathrm{m^2\cdot g^{-1}}$)		$\Delta S_{\mathrm{HA-S}}$ ($\mathrm{m^2\ g^{-1}}$)	$\Delta S'_{\mathrm{HA-S}}$ (%)
	before interaction	after interaction		
HA–S 14d	72.1	64.3	–7.8	–10.8
HA–S 28d	72.1	57.9	–14.2	–19.7
HA–S 42d	72.1	54.7	–17.4	–24.1
HA–S 56d	72.1	50.9	–21.2	–29.4

Records from a powder X-ray diffraction analysis (XRD) of HA–S were the same before and after individual time intervals of interaction with SBF. This is due to the chemical, as well as physical similarity of the synthetic hydroxyapatite HA–S and the newly developed phase HAp.

Figures 2 a-c show concentrations of Ca^{2+} and $(PO_4)^{3-}$ ions and pH values in SBF leachates depending on the time of interaction with HA–S.

Concentrations of ions in leachates reflect changes in behavior of the synthetic material almost immediately. After 2 hours after of the exposition of HA–S in SBF a sharp decrease of concentrations was observed for calcium ion (from 98 to 28 mg·l^{-1}) and phosphate ion (from 93 to 17.5 mg·l^{-1}) which suggests that the material surface was highly active for the nucleation of the new phase. Analyses of leachates have confirmed that precipitation of the new HAp phase occurred from the very beginning of the exposure. After 7 days the interaction between HA–S and the solution stabilized.

The reason may be the fact that it was mainly the newly developed HAp phase that reacted with SBF, as it was also observed on SEM images. The pH values were in conformity with the resulting changes of concentrations of ions analyzed in the leachates. After two hours of interaction with the HA–S material, pH decreased from 7.6 to 7.27. The pH then settled at 7.7 ± 0.3 and oscillated around that value until the end of the test.

Figure 3 shows the rate of formation of the new HAp phase on the surface of HA–S, i.e. relationship of weight of the developed HAp according to the Equation (4) on the interaction time. It is obvious that the rate of formation of the new HAp phase was linear throughout the entire time of interaction and nearly the same in all testing cells.

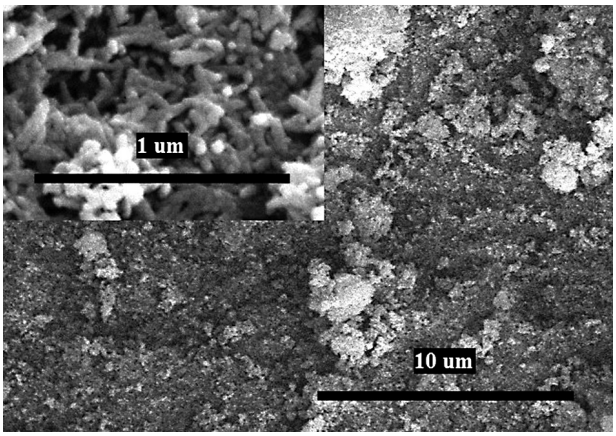

a) before interaction-origin

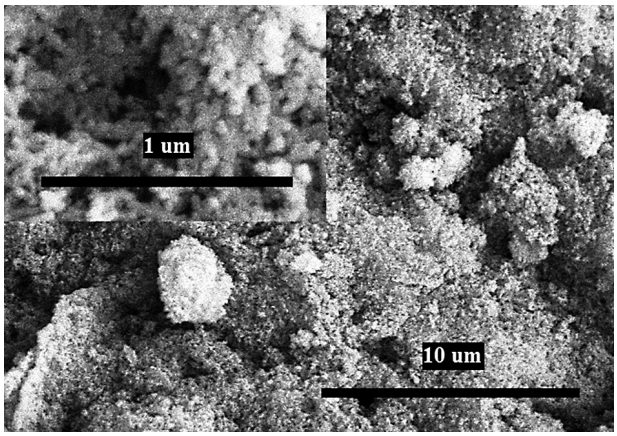

b) after 14 days

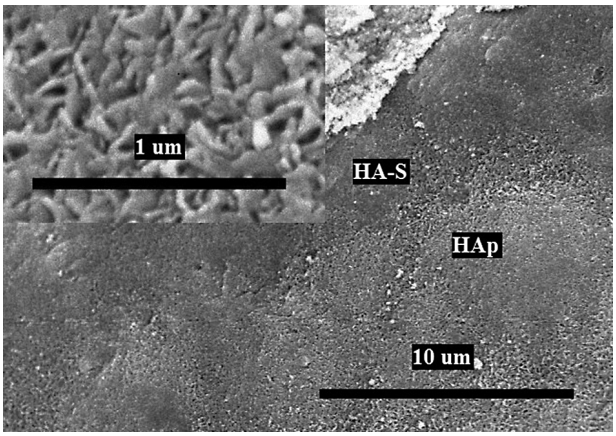

c) after 28 days

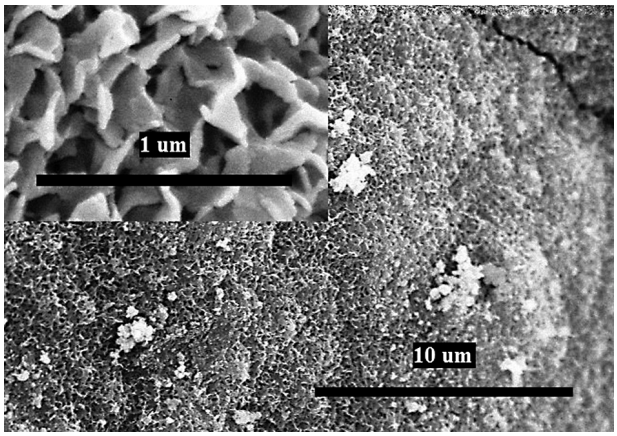

d) after 42 days

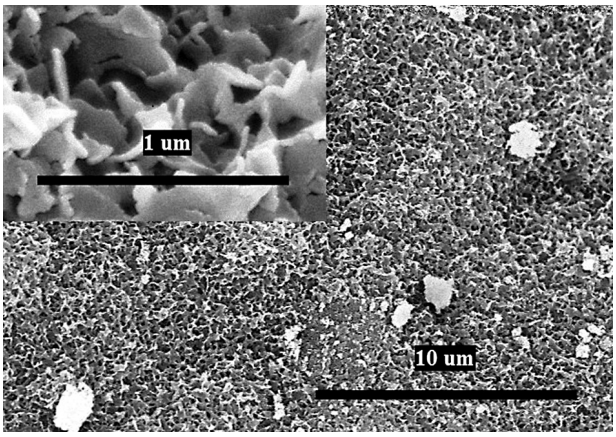

e) after 56 days

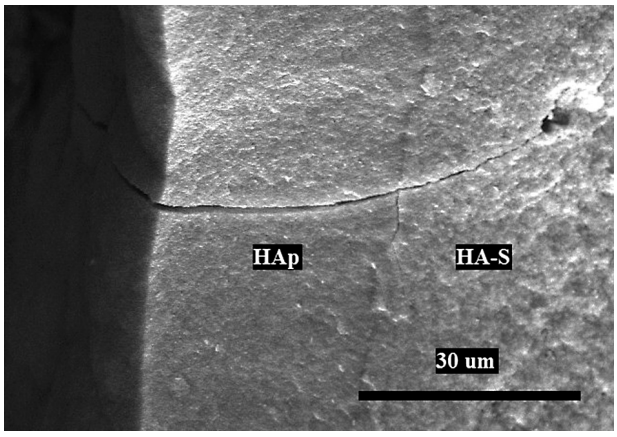

f) new HAp phase

Figure 1. SEM images of the material HA–S: a) before interaction-origin, b) after 14 days in SBF, c) after 28 days in SBF, d) after 42 days in SBF, e) after 56 days in SBF, f) detail of thickness of new HAp phase after 56 days in SBF.

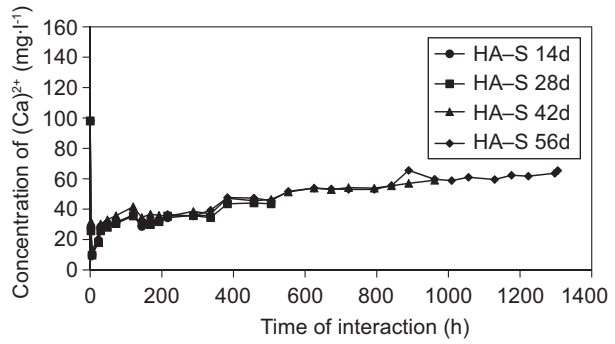

a) Ca^{2+}

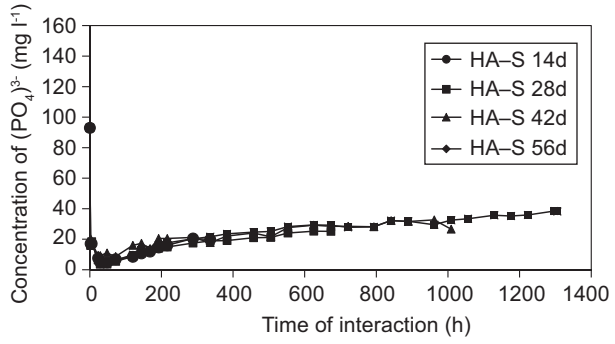

b) $(PO_4)^{3-}$

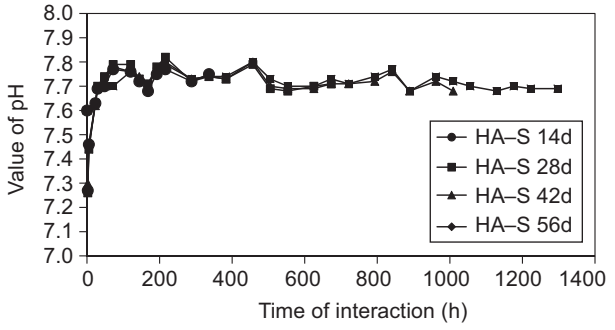

c) values of pH

Figure 2. Concentrations of a) Ca^{2+}, b) $(PO_4)^{3-}$ ions and c) values of pH in SBF during interaction with HA–S.

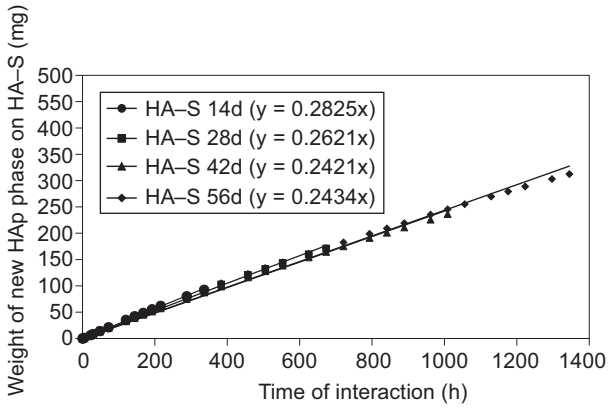

Figure 3. The weight of the new HAp phase on HA–S calculated from concentrations of $(PO_4)^{3-}$ ion during interaction with SBF.

Table 3 provides precipitation rates of the new HAp phase calculated from the growing weight of the material ($R_{m\ HA–S}$) and from the decrease of phosphate ion concentration in SBF ($R_{c\ HA–S}$) and their ratio ($R_{m\ HA–S}$/ $R_{c\ HA–S}$). The rate constants for the time periods were calculated using linear regression equations provided in (Figure 3).

Table 3. Rate of precipitation of the new HAp phase on the surface of HA–S after 14, 28, 42 and 56 days of interaction with SBF.

Material	$R_{m\ HA–S}$ (mg·hour^{-1})	$R_{c\ HA–S}$ (mg·hour^{-1})	$R_{m\ HA–S}/R_{c\ HA–S}$
HA–S 14d	0.332	0.282	1.177
HA–S 28d	0.294	0.262	1.122
HA–S 42d	0.258	0.242	1.066
HA–S 56d	0.258	0.243	1.061

Values shown in Table 3 clearly indicate that HA–S was reactive immediately after the beginning of the interaction with SBF. However, gradually, as the surface covered with the new phase, the rate of formation of the HAp phase slightly decreased. The ratio between the values $R_{m\ HA–S}$ and $R_{c\ HA–S}$ between day 14 and 28 was greater than 1. After 42 - 56 days the values of $R_{m\ HA–S}$ and $R_{c\ HA–S}$, obtained by two different methods of measurement ($R_{m\ HA–S}$ from weight of HA–S and $R_{c\ HA–S}$ from concentration of $(PO_4)^{3-}$ ion in SBF) stabilized and they were nearly identical (the ratio (R_m/R_c) was close to 1). The assumption that all $(PO_4)^{3-}$ ions removed from SBF were used to form HAp phase after day 42 has been confirmed.

Bovine hydroxyapatite HA–B

Also the weight of HA–B after the interaction with SBF (Table 4) increased with the interaction time. After 56 days of interaction the weight of HA–B increased in total by 76.5 %.

Table 4. The weights of material HA–B before and after 14, 28, 42 and 56 days of interaction with SBF.

Material	Weight (g) before interaction	Weight (g) after interaction	$\Delta m_{HA–B}$ (g)	$\Delta m'_{HA–B}$ (%)
HA–B 14d	0.375	0.468	+0.093	+24.8
HA–B 28d	0.375	0.542	+0.167	+44.5
HA–B 42d	0.375	0.609	+0.234	+62.4
HA–B 56d	0.375	0.662	+0.287	+76.5

The original material before the interaction with SBF is in Figure 4a. Figures 4b-f show the surfaces of HA–B after specific periods of time of the interaction.

Figure 4b indicates that as early as during the first 14 days the surface of HA–B covered with the new phase made of nanocrystalline plates of hydroxyapatite (HAp). The phase filled macro and micro pores of HA–B and the nanocrystals gradually formed a continuous layer. A cracked layer made up of globules of aggregated nanocrystals, typical for the newly formed hydroxyapatite (HAp), is well visible when a smaller resolution is used (Figure 4f). The HA–B surface covered with the newly formed HAp phase in a shorter period of time (14 days) in comparison with the synthetic material HA–S, for which it took approximately 28 days. A comparison of SEM/EDS images of both the materials shows that the surface of synthetic HA–S started to cover with nanoplates of HAp on the day 14 of the interaction and on day 28 it was covered completely.

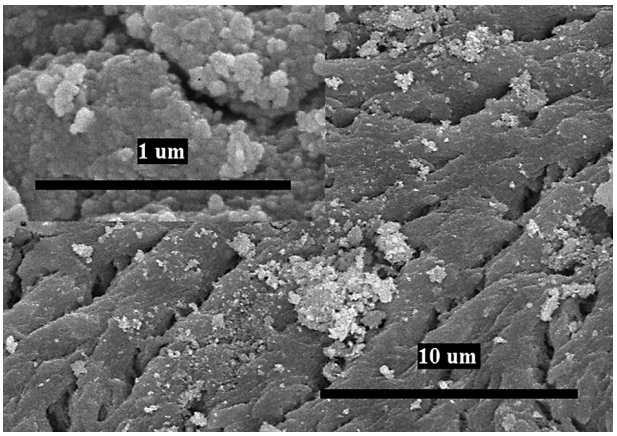

a) before interaction-origin

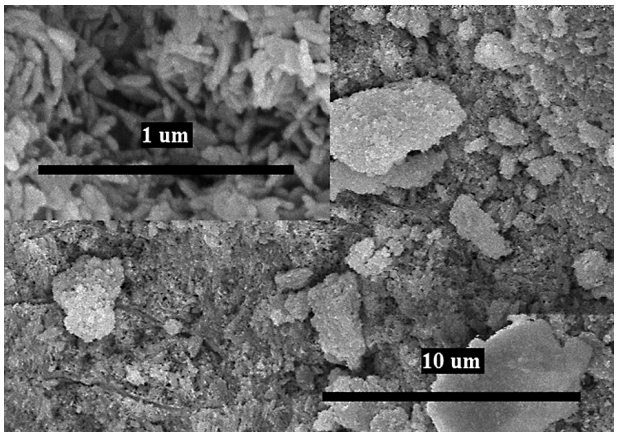

b) after 14 days

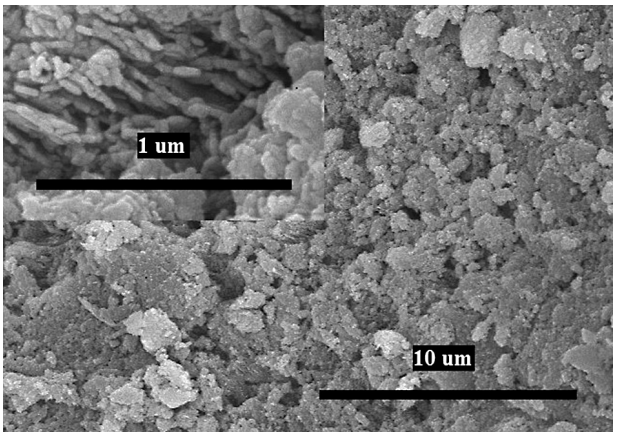

c) after 28 days

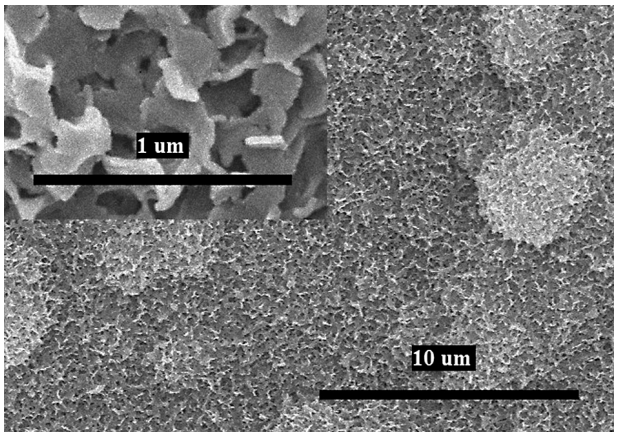

d) after 42 days

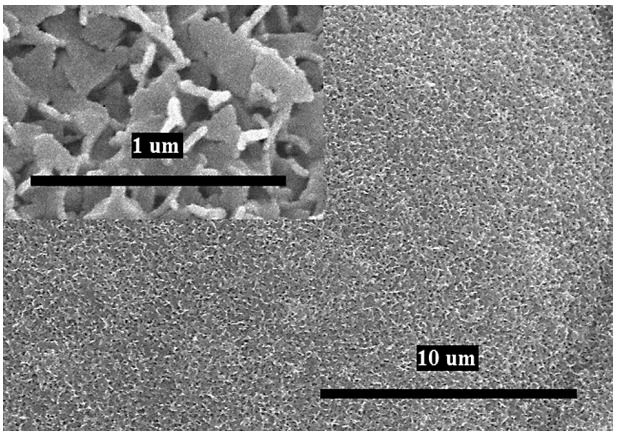

e) after 56 days

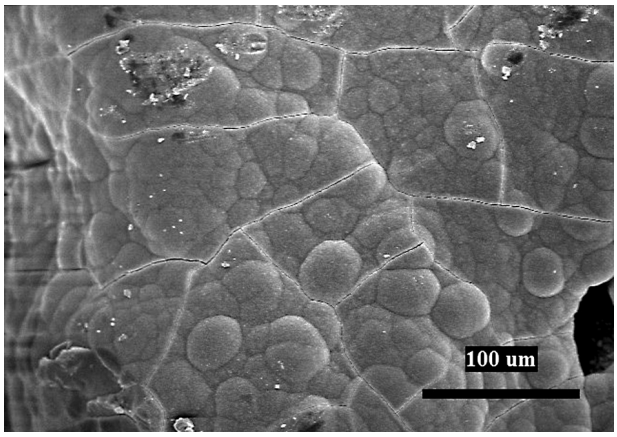

f) new HAp phase

Figure 4. SEM image of the material HA–B: a) before interaction- origin, b) after 14 days in SBF, c) after 28 days in SBF, d) after 42 days in SBF, e) after 56 days in SBF, f) surface of new HAp phase after 56 days in SBF.

After 14 days of exposure a decrease of the specific surface (Table 5) was observed. After 56 days the specific surface of bovine hydroxyapatite HA–B decreased from the original 94.4 $m^2.g^{-1}$ to 52.4 $m^2 \cdot g^{-1}$, i.e. to values similar to that of HA–S (50.9 $m^2 \cdot g^{-1}$).

Table 5. The values of specific surface of material HA–B before and after 14, 28, 42 and 56 days of interaction with SBF.

Material	Specific surface ($m^2 \cdot g^{-1}$) before interaction	Specific surface ($m^2 \cdot g^{-1}$) after interaction	ΔS_{HA-B} ($m^2\ g^{-1}$)	$\Delta S'_{HA-B}$ (%)
HA–B 14d	94.4	75.9	–18.5	–19.6
HA–B 28d	94.4	63.7	–30.6	–32.4
HA–B 42d	94.4	56.9	–37.4	–39.6
HA–B 56d	94.4	52.4	–42.0	–44.5

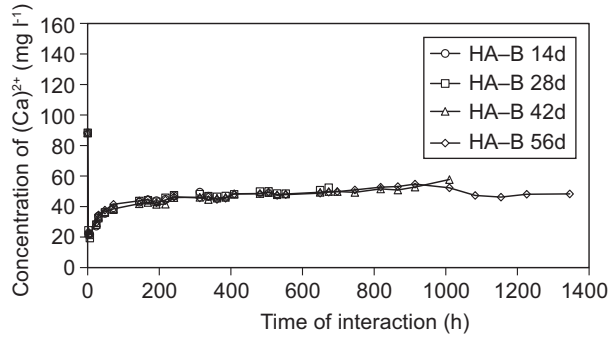

a) Ca^{2+}

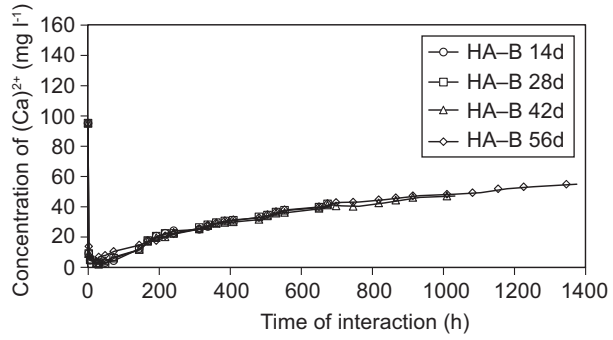

b) $(PO_4)^{3-}$

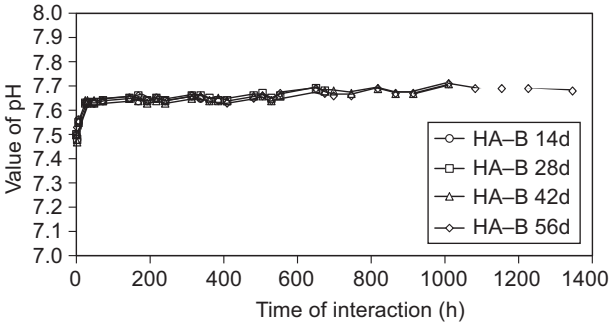

c) values of pH

Figure 5. Concentrations of a) Ca^{2+}, b) $(PO_4)^{3-}$ ions and c) values of pH in SBF during interaction with HA–B.

The XRD method did not succeed to differentiate between the original bovine hydroxyapatite HA–B and the newly formed HAp phase. The reason (equally as for the previous HA–S material) was their chemical and phase similarity (Ref. Code: 01-074-0566).

Figure 5 show concentrations of Ca^{2+} and $(PO_4)^{3-}$ ions and pH values in SBF leachates depending on the time of interaction with HA–B.

Two hours after the beginning of interaction a sharp drop of concentrations occurred for both the ions, which suggests an immediate reaction of the material with SBF. In the case of $(PO_4)^{3-}$ ion it dropped nearly to zero. After 7 days the concentration of Ca^{2+} stabilized, the concentration of $(PO_4)^{3-}$ after the initial dramatic decrease gradually grew and the trend persisted until the end of the experiment. Changes of concentrations of Ca^{2+} and $(PO_4)^{3-}$ ions with time in SBF for bovine hydroxyapatite HA–B were similar those found in case of synthetic hydroxyapatite HA–S. The pH values slightly increased after two hours of interaction and remained nearly constant until the end of the experiment.

Figure 6 shows the rate of formation of the new HAp phase on the surface of HA–B throughout the entire 56 days of interaction with SBF (according to the equation (4)). The rate of formation of the new HAp phase on the surface of HA–B was nearly identical in all the testing cells.

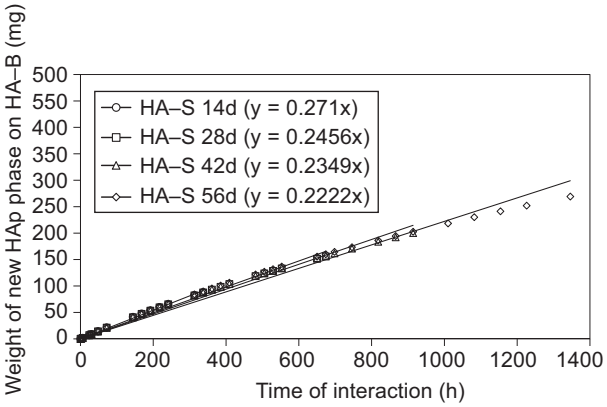

Figure 6. The weight of the new HAp phase on HA–B calculated from concentrations of $(PO_4)^{3-}$ ions during interaction with SBF.

Table 6 shows precipitation rates of the new HAp phase on the surface of HA–B calculated, equally as for the previous material, from the increased weight of HA–B ($R_{m\ HA-B}$) and from the decrease of $(PO_4)^{3-}$ ions concentration in SBF leachates ($R_{c\ HA-B}$) and their ratio ($R_{m\ HA-B}/R_{c\ HA-B}$). The rate constants for the time periods were calculated using linear regression equations provided in (Figure 6).

Values shown in Table 6 indicate that bovine hydroxyapatite HA–B is also highly reactive from the beginning of exposure to SBF and the rate of formation of the new HAp phase ($R_{m\ HA-B}$) slightly decreases with time.

Values of the rates ($R_{m\,HA–B}$ and $R_{c\,HA–B}$) for bovine HA–B were obtained by two different methods: the change of weight of HA–B and from concentration of $(PO_4)^{3-}$ ions in SBF. From the beginning of exposure these values were nearly the same. The assumption that all $(PO_4)^{3-}$ removed from SBF were used to form HAp has been confirmed.

Table 6. Rate of precipitation of the new HAp phase on the surface of HA–B after 14, 28, 42 and 56 days of interaction with SBF.

Material	$R_{m\,HA–B}$ (mg·hour^{-1})	$R_{c\,HA–B}$ (mg·hour^{-1})	$R_{m\,HA–B}/R_{c\,HA–B}$
HA–B 14d	0.279	0.271	1.029
HA–B 28d	0.248	0.246	1.008
HA–B 42d	0.232	0.232	1.000
HA–B 56d	0.213	0.222	0.959

Comparison of synthetic and bovine hydroxyapatite

For the comparison of relative coverage of HA–S and HA–B materials with the new HAp phase it is necessary to take into account their original weights and original specific surfaces according to equations (5) and (6). It is obvious that, due to the different initial weights and specific surfaces, the surfaces area of the materials were nearly the same ($A_{HA–S}$ = 36.1 m^2, $A_{HA–B}$ = 35.4 m^2). When comparing synthetic and bovine hydroxyapatites in terms of their changing weights, $\Delta m'$ (Tables 1 and 4), we can conclude that the trends found for both the materials were similar. In this comparison (Figure 7) bovine HA–B seemed slightly more reactive than synthetic HA–S. The weight of HA–B grew almost linearly from the beginning of exposure. For synthetic HA–S we observed a slight slowdown of formation of the new phase after the 28th day of exposure.

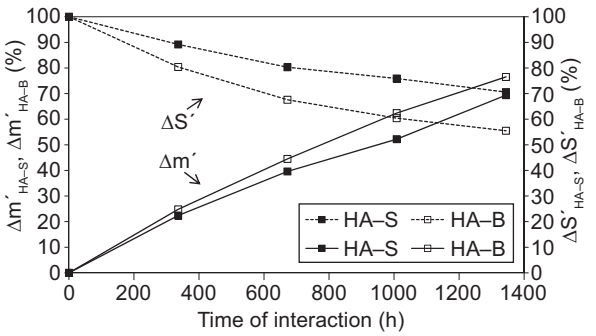

Figure 7. Comparison of the weight and the specific surface difference of material HA–S and HA–B during interaction with SBF.

A more significant difference between the tested materials was observed for the specific surface. The percentage change ΔS´ of HA–S was smaller than that of HA–B (Tables 2 and 5). However, the trends of the ΔS´ decrease were again the same for both the materials (Figure 7).

The assumption that all $(PO_4)^{3-}$ ions removed from the SBF are consumed for the formation of HAp (according to R_c calculation) was found correct for HA–S after day 42 and from the very beginning of the interaction for HA–B. It is probable that either non-stoichiometric HAp or amorphous calcium phosphate (ACP) develops on synthetic HA–S during the interval of 0 - 42 days. After day 42 the ratios R_m/R_c were nearly the same (value 1) for both materials. For clinical using could be interesting information that 0.5 g of synthetic HA–S and 0.375 g of bovine HA–B material provide the same surface area (A) and the bulk density (materials filled exactly ¼ of the testing cell volume). This study indicates that the both HA materials cause the formation of the Ca-P phase immediately after application. The newly formed phase has amorphous character (probably ACP) in the case of the synthetic HA–S. Gradually, HAp crystals are formed on the HA–S surface (28 days after interaction). The crystalline HAp was formed on the surface of the bovine HA–B from the beginning of the exposition and the crystals very quickly covered the original surface. The newly formed crystalline layer could reduce further remodelling of the bovine HA–B.

CONCLUSION

The SEM/EDS measurements have shown that granules of synthetic HA–S started covering with the newly formed HAp phase ca. 14 days later than granules of bovine HA–B. Both materials were completely covered with the new well developed HAp phase and also the rates of its formation were similar on the day 42 of the immersion in SBF. Therefore SBF further reacted probably only with the newly developed HAp phase on the surface of the both materials under our experimental conditions. Our model, which assumes that all $(PO_4)^{3-}$ ions removed from SBF precipitated on the tested material surface to form HAp, can be used for bovine HA–B throughout the entire time of interaction and for the synthetic HA–S after the 42th day of interaction. It is probable that, at the beginning of the exposure, an amorphous calcium phosphate phase (ACP) develops on the surface of synthetic HA–S instead of HAp phase. The tested materials were identical hydroxyapatites, in terms of their chemical composition, crystallinity and even with the same reaction surface area. In spite of different way of preparation, the weight and the specific surface, the granules of synthetic and bovine hydroxyapatites react very similar with SBF in second period of our experiment.

Acknowledgements

This work was supported by the Technology Agency for the Czech Republic within the project TE01020390 Center for development of modern metallic biomaterials for medicinal implants. We thank Dr. Petr Bezdička for XRD measurement and Ing. Miloslav Lhotka Ph.D. for BET measurement.

References

1. Cao W., Hench L.L.: Ceram. Inter. *22*, 493 (1996).
2. Best S.M., Porter A.E., Thian E.S., Huang J.: J. Eu. Ceram. Soc. *28*, 1319 (2008).
3. Dorozhkin S.V.: Materials *2*, 1975 (2009).
4. Dorozhkin S.V.: Acta Biomaterialia *6*, 4457 (2010).
5. El Hammari L., Merroun H., Coradin T., Cassaignon S., Laghzizil A., Saoiabi A.: Mater. Chem. Phys. *104*, 448 (2007).
6. Cao L-y., Zhang Ch-b., Huang J-f.: Ceram. Inter. *31*, 1041 (2005).
7. Kweh S.W.K., Khor K.A., Cheang P.: J. Mater. Proces. Tech. *89-90*, 373 (1999).
8. Mostafa N.Y.: Mater. Chem. Phys. *94*, 333 (2005).
9. Fathi M.H., Hanifi A.: Materials Letters *61*, 3978 (2007).
10. Bezzi G., Celotti G., Landi E., La Torretta T.M.G., Sopyan I., Tampieri A.: Mater. Chem. Phys. *78*, 816 (2003).
11. Wang F., Li M.S., Lu Y.P., Qi Y.X.: Materials Letters *59*, 916 (2005).
12. Rhee S.H.: Biomaterials *23*, 1147 (2002).
13. Yeong K.C.B., Wang J., Ng S.C.: Biomaterials *22*, 2705 (2001).
14. Pramanik S., Agarwal A.K., Rai K.N., Garg A.: Ceram. Inter. *33*, 419 (2007).
15. Ruksudjarit A., Pengpat K., Rujijanagul G., Tunkasiri T.: Cur. Ap. Phys. *8*, 270 (2008).
16. Ooi C.Y., Hamdi M., Ramesh S.: Ceram. Inter. *33*, 1171 (2007).
17. Herliansyah M.K., Hamdi M., Ide-Ektessabi A., Wildan M.W., Toque J.A.: Mater. Sci. Eng. *C29*, 1674 (2009).
18. Dorozhkin S.V.: Prog. Crys. Gro. Char. Mater. *45*, (2002).
19. Christoffersen J., Christoffersen M.R., Kjaergaard N.: J. Cryst. Gro. *43*, 501 (1978).
20. Christoffersen J., Christoffersen M.R.: J. Crysy. Gro. *53*, 42 (1981).
21. Kokubo T., Takadama H.: Biomaterials *27*, 2907 (2006).
22. Kokubo T., Kim H-M., Kawashita M.: Biomaterials *24*, 2161 (2003).
23. Kim H-M., Himeno T., Kokubo T., Nakamura T.: Biomaterials *26*, 4366 (2005).
24. Bohner M., Lemaitre J.: Biomaterials *30*, 2175 (2009).
25. Helebrant A., Jonášová L., Šanda L.: Ceram.-Sil. *46*, 9 (2002).
26. Horkavcová D., Zítková K., Rohanová D., Helebrant A., Cílová Z.: Ceram.-Sil. *54*, 398 (2010).
27. Rohanová D., Boccaccini A.R., Yunos D.M., Horkavcová D., Březovská I., Helebrant A.: Acta Biomaterialia *7*, 2623 (2011).